Light scattering from an amplifying medium bounded by a randomly rough surface: A numerical study

Ingve Simonsen,[1,2] Tamara A. Leskova,[3] and Alexei A. Maradudin[2]
[1]*Department of Physics, The Norwegian University of Science and Technology, Trondheim, Norway*
[2]*Department of Physics and Astronomy and Institute for Surface and Interface Science, University of California, Irvine, California 92697*
[3]*Institute of Spectroscopy, Russian Academy of Sciences, Troitsk 142092, Russia*
(Received 29 August 2000; published 29 June 2001)

By numerical simulations we study the scattering of *s*-polarized light from a rough dielectric film deposited on the planar surface of a semi-infinite perfect conductor. The dielectric film is allowed to be either active or passive, situations that we model by assigning negative and positive values, respectively, to the imaginary part ε_2 of the dielectric constant of the film. We study the reflectance $\mathcal{R}$ and the total scattered energy $\mathcal{U}$ for the system as functions of both ε_2 and the angle of incidence of the light. Furthermore, the positions and widths of the enhanced backscattering and satellite peaks are discussed. It is found that these peaks become narrower and higher when the amplification of the system is increased, and that their widths are linear functions of ε_2. The positions of the backscattering peaks are found to be independent of ε_2, while we find a weak dependence on this quantity in the positions of the satellite peaks.

DOI: 10.1103/PhysRevB.64.035425 PACS number(s): 42.25.Dd, 42.25.Bs

I. INTRODUCTION

In the first half of the 1990s and subsequently, amplifying volume disordered media received a great deal of attention from theorists[1,2] and experimentalists[2,3] alike. This attention was partly motivated by the suggestion of using random volume scattering media to construct a so-called random laser.[4] For scattering systems possessing surface disorder in contrast to volume disorder, the overwhelming majority of theoretical and experimental studies were devoted to scattering from passive (i.e., absorbing) media. Only recently has the surface scattering community begun study surface-disordered amplifying systems. The only literature on the scattering of light from amplifying surface-disordered media known to us is the theoretical study by Tutov *et al.*[5] and the experimental investigation by Gu and Peng.[6] In the theoretical work by Tutov *et al.*,[5] the authors conducted a perturbative study of the scattering of *s*-polarized light from an amplifying film deposited on the planar surface of a perfect conductor, where the vacuum-film interface was a one-dimensional random interface characterized by a Gaussian power spectrum. In this work we consider the same scattering system, but apply a numerical simulation approach for its study. The numerical approach is based on the solution of the reduced Rayleigh equation that the scattering amplitude for the system satisfies. The use of a numerical simulation approach enables us to study possible nonperturbative effects[7] that could not be accounted for by the perturbative technique used in Ref. 5. Furthermore, we also use a different power spectrum of the surface roughness. In particular, a West-O'Donnell (or rectangular) power spectrum[8] is used in this work, in contrast to the Gaussian power spectrum used by Tutov *et al.* Such a power spectrum allows for the suppression of single scattering over a range of scattering angles and, more importantly, it opens the possibility for a strong coupling of the incident light to guided waves supported by the film structure.

In this work we calculate the reflectivity of a surface-random vacuum-dielectric-metal film geometry, illuminated from above by *s*-polarized light of frequency ω. The metal-dielectric interface is assumed to be flat, while the vacuum-dielectric interface is described by the surface profile function $\zeta(x_1)$. The amplifying medium (i.e., the film) is modeled by a dielectric medium whose dielectric constant ε has an imaginary part ε_2 that is negative, while its real part ε_1 is positive. The values of ε_2 are chosen so that they include gains $[g=2\pi|\varepsilon_2|/(\lambda\sqrt{\varepsilon_1})]$ in the medium that are physically realizable. The assumption of a negative imaginary part to ε is the simplest way of modeling stimulated emission in this system. The reflectivity is given by $|R(k)|^2$, where $R(k)$ is defined in terms of the scattering amplitude $R(q|k)$ by $|\langle R(q|k)\rangle|^2 = L_1 2\pi\delta(q-k)|R(k)|^2$. In this relation the wave numbers k and q are related to the angles of incidence and scattering by $k=(\omega/c)\sin\theta_0$ and $q=(\omega/c)\sin\theta_s$, respectively, L_1 is the length of the x_1 axis covered by the random surface, and the angular brackets denote an average over the ensemble of realizations of the surface profile function $\zeta(x_1)$. The scattering amplitude $R(q|k)$ is obtained by numerically solving the reduced Rayleigh equation it satisfies for a large number of realizations of $\zeta(x_1)$, and $\langle R(q|k)\rangle$ is obtained by averaging the results. As expected, the reflectivity of the amplifying medium with a random surface is larger than that of the corresponding absorbing medium, viz. a medium with the same value of $|\varepsilon_2|$ but with ε_2 positive, for all angles of incidence.

II. SCATTERING THEORY

A. Scattering system

The scattering system that will be considered in this paper consists of a dielectric film, with a randomly rough top interface, deposited on the planar surface of a semi-infinite perfect conductor. In particular, it consists of a vacuum in

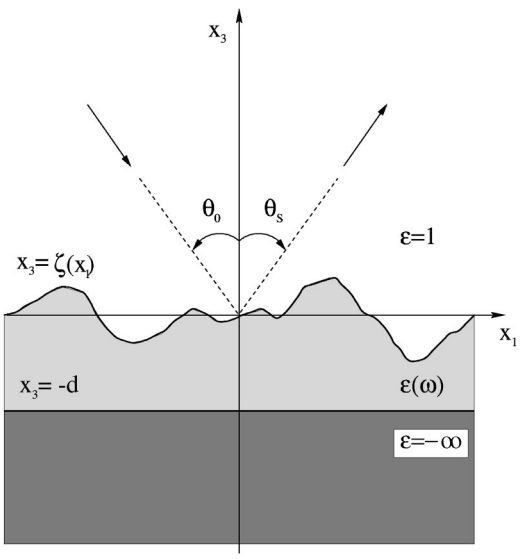

FIG. 1. The scattering geometry considered in the present work.

the region $x_3 > \zeta(x_1)$, an amplifying or absorbing dielectric medium in the region $-d < x_3 < \zeta(x_1)$, and a perfect conductor in the region $x_3 < -d$. This geometry is depicted in Fig. 1. The rough surface profile function, denoted by $\zeta(x_1)$, is assumed to be a single-valued function of its argument, and is differentiable as many times as needed. Furthermore, it is assumed to constitute a zero-mean, stationary, Gaussian random process defined by

$$\langle \zeta(x_1) \rangle = 0, \tag{2.1a}$$

$$\langle \zeta(x_1)\zeta(x_1') \rangle = \delta^2 W(|x_1 - x_1'|), \tag{2.1b}$$

where $\langle \cdot \rangle$ denotes an average over the ensemble of realizations of $\zeta(x_1)$, and δ is the rms height of the rough surface. Moreover, $W(|x_1|)$ denotes the surface height autocorrelation function, and is related to the power spectrum of the surface roughness $g(|k|)$ by

$$g(|k|) = \int_{-\infty}^{\infty} dx_1 W(|x_1|) \; e^{-ikx_1}. \tag{2.2}$$

In the numerical simulation results to be presented later, we will assume a rectangular power spectrum, also known as the West-O'Donnell form,

$$g(|k|) = \frac{\pi}{k_+ - k_-}[\theta(k - k_-)\theta(k_+ - k) + \theta(-k_- - k)\theta(k + k_+)], \tag{2.3}$$

where $\theta(k)$ is the Heaviside unit step function, and $k_\pm$ are parameters to be specified. This power spectrum was recently used in an experimental study of enhanced backscattering from weakly rough surfaces.[8]

B. Scattering equations

If the vacuum-dielectric interface $x_3 = \zeta(x_1)$ is illuminated from the vacuum side by an s-polarized electromagnetic wave of frequency ω, the only nonzero component of the electric field vector in the region $x_3 > \zeta(x_1)_{max}$ is the sum of an incident wave and a scattered field:

$$E_2^>(x_1, x_3|\omega) = e^{ikx_1 - i\alpha_0(k,\omega)x_3} + \int_{-\infty}^{\infty} \frac{dq}{2\pi} R(q|k) e^{iqx_1 + i\alpha_0(q,\omega)x_3}. \tag{2.4}$$

In this equation $R(q|k)$ denotes the scattering amplitude, while we have defined

$$\alpha_0(q,\omega) = \begin{cases} \sqrt{\dfrac{\omega^2}{c^2} - q^2}, & |q| < \omega/c \\ i\sqrt{q^2 - \dfrac{\omega^2}{c^2}}, & |q| > \omega/c. \end{cases} \tag{2.5}$$

From a knowledge of the scattering amplitude one can define the differential reflection coefficient (DRC) $\partial R/\partial \theta_s$. It is defined such that $(\partial R/\partial \theta_s) d\theta_s$ is the fraction of the total time-averaged flux incident on the surface that is scattered into the angular interval $d\theta_s$ about the scattering angle θ_s, in the limit as $d\theta_s \to 0$. The contribution to the mean differential reflection coefficient from the coherent (specular) component of the scattered field is given by[9,10]

$$\left\langle \frac{\partial R}{\partial \theta_s} \right\rangle_{\text{coh}} = \frac{1}{L_1} \frac{\omega}{2\pi c} \frac{\cos^2\theta_s}{\cos\theta_0} |\langle R(q|k) \rangle|^2, \tag{2.6a}$$

and the contribution to the mean differential reflection coefficient from the incoherent (diffuse) component of the scattered field is given by[9,10]

$$\left\langle \frac{\partial R}{\partial \theta_s} \right\rangle_{\text{incoh}} = \frac{1}{L_1} \frac{\omega}{2\pi c} \frac{\cos^2\theta_s}{\cos\theta_0} [\langle |R(q|k)|^2 \rangle - |\langle R(q|k) \rangle|^2]. \tag{2.6b}$$

In Eqs. (2.6), L_1 is the length of the x_1 axis covered by the random surface, and the wave numbers k and q are related to the angles of incidence θ_0 and the angle of scattering θ_s according to

$$k = \frac{\omega}{c} \sin\theta_0, \quad q = \frac{\omega}{c} \sin\theta_s. \tag{2.7}$$

Both these angles are measured from the normal to the mean surface, as indicated in Fig. 1.

From the definition of the mean differential reflection coefficient, we find that the reflectance of the surface is defined according to

$$\mathcal{R} = \int_{-\pi/2}^{\pi/2} d\theta_s \left\langle \frac{\partial R}{\partial \theta_s} \right\rangle_{\text{coh}} = |R(k)|^2, \tag{2.8}$$

where k is given by Eq. (2.7), and $R(k)$ is related to the scattering amplitude $|R(q|k)|^2$ by $|\langle R(q|k) \rangle|^2 = L_1 2\pi\delta(q - k)|R(k)|^2$. Likewise, the total scattered energy (normalized to the incident energy) is defined by

$$\mathcal{U}=\int_{-\pi/2}^{\pi/2} d\theta_s \left\langle \frac{\partial R}{\partial \theta_s} \right\rangle, \tag{2.9}$$

where $\langle \partial R/\partial \theta_s \rangle$ is the total mean DRC, i.e., the sum of the coherent and incoherent contribution as defined in Eqs. (2.6a) and (2.6b), respectively.

So far we have not specified how to obtain the scattering amplitude entering into the above equations. It has previously been shown that $R(q|k)$ is the solution of the so-called reduced Rayleigh equation.[11] This single, inhomogeneous integral equation for $R(q|k)$ for our scattering geometry reads[10]

$$\int_{-\infty}^{\infty} \frac{dq}{2\pi} M(p|q)R(q|k)=N(p|k), \tag{2.10a}$$

where

$$M(p|q)=\frac{e^{i\alpha(p,\omega)d}}{\alpha_0(q,\omega)+\alpha(p,\omega)} I[\alpha_0(q,\omega)+\alpha(p,\omega)|p-q] - \frac{e^{-i\alpha(p,\omega)d}}{\alpha_0(q,\omega)-\alpha(p,\omega)} I[\alpha_0(q,\omega) - \alpha(p,\omega)|p-q], \tag{2.10b}$$

$$N(p|k)=-\frac{e^{i\alpha(p,\omega)d}}{\alpha(p,\omega)-\alpha_0(k,\omega)} I[\alpha(p,\omega)-\alpha_0(k,\omega)|p-k] - \frac{e^{-i\alpha(p,\omega)d}}{\alpha(p,\omega)+\alpha_0(k,\omega)} I[-\alpha(p,\omega) - \alpha_0(k,\omega)|p-k], \tag{2.10c}$$

with

$$I(\gamma|q)=\int_{-\infty}^{\infty} dx_1 e^{i\gamma\zeta(x_1)} e^{-iqx_1}. \tag{2.10d}$$

In writing Eq. (2.10), we have introduced

$$\alpha(q,\omega)=\sqrt{\varepsilon(\omega)\frac{\omega^2}{c^2}-q^2}, \tag{2.11}$$

where the branch of the square root is chosen so that the real part of $\alpha(q,\omega)$ is always positive, while the imaginary part is positive when $\varepsilon_2>0$, but is negative when $\varepsilon_2<0$.

The simulation results to be presented in Sec. III were obtained by directly solving numerically the reduced Rayleigh equation (2.10). This approach can treat much longer rough surfaces as compared to a rigorous numerical simulation approach[9] with the same use of computer power and memory. An additional advantage of a numerical approach based on the reduced Rayleigh equation is that $\mathcal{R}$ and $\mathcal{U}$ can be calculated to high precision, whereas the same quantities calculated by a rigorous approach have been found to be less accurate for the surface lengths typically used in such simulations. We believe this difference in accuracy for $\mathcal{R}$ and $\mathcal{U}$ for these two numerical approaches is related to the difference in the length of the surface that can be handled practically with today's typical computer resources. The numerical solution of the reduced Rayleigh equation is done by converting the integral equation into a set of linear equations obtained by using an appropriate quadrature scheme and solving the resulting system by standard numerical techniques.[12] Due to the increased numerical performance, the calculation of the $I(\gamma|q)$ integrals was based on an expansion of the integrand in powers of the surface profile function. This numerical method was recently applied successfully to a similar scattering geometry[7], and the interested reader is directed to this paper for details of the numerical method.

III. RESULTS AND DISCUSSIONS

For the numerical simulations to be presented below, we have considered the scattering of *s*-polarized incident light of wavelength $\lambda=632.8$ nm. The film was assumed to have a mean thickness $d=500$ nm, and its dielectric constant at the wavelength of the incident light was taken to be $\varepsilon(\omega)=2.6896+i\varepsilon_2$, where ε_2 is allowed to vary over both positive and negative values. The surface profile function was characterized by a power spectrum of the West-O'Donnell type as defined in Eq. (2.3). For the parameters defining the power spectrum, we used $k_-=0.86\,\omega/c$ and $k_+=1.97\,\omega/c$. For these values of $k_\pm$, single scattering should be suppressed for scattering angles in the range $|\theta_s|<55.1°$. The rms height of the surface was taken to be $\delta=30$ nm. Furthermore, the length of the surface was taken to be $L=160\lambda$, and the numerical results were all averaged over $N_\zeta=3000$ realizations of the surface profile function.

In Fig. 2(a) we present the numerical simulation results for the contribution to the mean differential reflection coefficient from the light that has been scattered incoherently, $\langle \partial R/\partial \theta_s \rangle_{\text{incoh}}$, for *s*-polarized light incident normally on the mean surface ($\theta_0=0°$). The values of the imaginary part of the dielectric were (from top to bottom) $\varepsilon_2=-0.0025$, 0, and 0.0025. From this figure we note the enhanced backscattering peaks located at $\theta_s=\theta_0=0°$. Moreover, two satellite peaks, located symmetrically about the position of the enhanced backscattering peak, are easily distinguished from the background. Their positions, as read from Fig. 2(a), fit nicely with their positions, $\theta_\pm=\pm 17.7°$, calculated for the corresponding planar geometry in the limit of vanishing ε_2[7]. The choices made for ε_2 of the film in Fig. 2(a) correspond to an amplifying or active film ($\varepsilon_2=-0.0025$), a neither amplifying nor absorbing film ($\varepsilon_2=0$), and an absorbing or passive film ($\varepsilon_2=0.0025$), respectively. This is reflected in Fig. 2(a), where the contribution to the mean DRC from the light scattered incoherently from the amplifying medium is larger for all scattering angles than for the other two cases, due to the extra energy gained by the scattered light from the amplifying film. Moreover, it is interesting to note that the differences between these curves are largest for small scattering angles, and as one moves to larger scattering angles these differences are reduced. The main reason for this is that for scattering angles $|\theta_s|<55.1°$ the light undergoes multiple

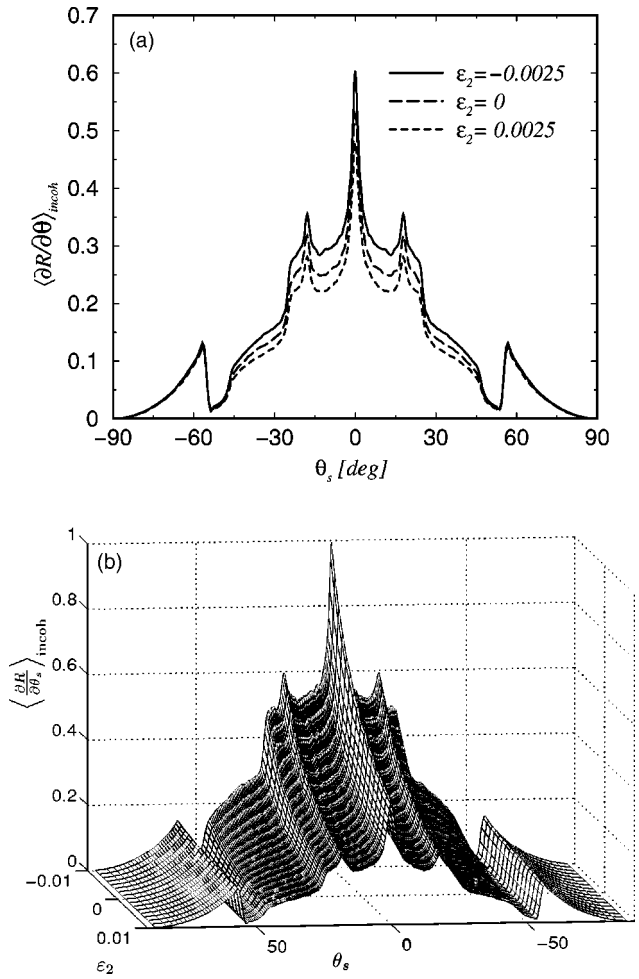

FIG. 2. The mean differential reflection coefficient for the incoherently scattered light for (a) $\varepsilon_2 = 0, \pm 0.0025$, and (b) as a function of the same parameter. For both figures the angle of incidence was $\theta_0 = 0°$, and the wavelength of the incident light was $\lambda = 632.8$ nm. The dielectric constant of a film of mean thickness $d = 500$ nm was $\varepsilon(\omega) = 2.6896 + i\varepsilon_2$, where ε_2 is as indicated in the figure. The randomly rough surface had a rms roughness of $\delta = 30$ nm. The power spectrum was of the West-O'Donnell type defined by the parameters $k_- = 0.86\,\omega/c$ and $k_+ = 1.97\,\omega/c$.

scattering, which will increase the effects of amplification and absorption as compared to a system that is dominated by single-scattering events for such scattering angles. In the wings of the angular dependence of the mean DRC, $|\theta_s| > 55.1°$, where single scattering gives the main contribution, the differences between the curves corresponding to different values of ε_2 is much less pronounced. In order to obtain a more complete picture of how the incoherent component of the mean DRC depends on the imaginary part of the dielectric function, in Fig. 2(b) we present a plot showing $\langle \partial R/\partial\theta_s \rangle_{\rm incoh}$ as a function of ε_2, as well as of the scattering angle θ_s. The angle of incidence here was also chosen to be $\theta_0 = 0°$. As seen from this plot, the positions of the peaks are fixed, or close to fixed, while the overall amplitude of $\langle \partial R/\partial\theta_s \rangle_{\rm incoh}$ increases monotonically with the decreasing imaginary part of the dielectric constant.

To quantify better how the amplification or absorption depends on ε_2, we have studied the total energy scattered by the surface as well as its reflectance. These two quantities, denoted by $\mathcal{U}(\theta_0, \varepsilon_2)$ and $\mathcal{R}(\theta_0, \varepsilon_2)$ respectively, are related to the mean differential reflection coefficient by Eqs. (2.8) and (2.9). The numerical results for these two quantities for normal incidence are given in Figs. 3(a) and 3(b). For small values of ε_2 we find that these quantities are linear in ε_2. However, when the absolute value of the imaginary part of the dielectric constant increases, a deviation from this behavior is observed. The numerical data in both cases are well fitted by a cubic polynomial in ε_2. In Fig. 3(c) we present the numerical results for $\mathcal{U}$ and $\mathcal{R}$ as a function of the angle of incidence θ_0 for $\varepsilon_2 = \pm 0.0025$. It is seen that $\mathcal{U}(\theta_0)$ is a monotonically increasing or decreasing function of the angle of incidence for positive and negative values of ε_2, respectively, and the two curves for $\varepsilon_2 = \pm 0.0025$ are symmetric with respect to the line $\mathcal{U}(\theta_0) = 1$. For negative (positive) ε_2 the total scattered energy is larger (smaller) than unity. However, from the same graph it is observed that $\mathcal{R}(\theta_0)$ is not a monotonic function of ε_2. Instead it has a minimum in the vicinity of 25°. Below this value it is decreasing, while above it is increasing. The reason for this behavior is due to the excitation of a leaky guided wave supported by the scattering geometry.[5] The minimum in $\mathcal{R}(\theta_0)$ occurs for an angle of incidence corresponding to the wave number of the leaky guided wave, and the excitation of this mode will take away scattered energy from the specular direction, resulting in a minimum in $\mathcal{R}(\theta_0, \varepsilon_2)$ for this angle of incidence.

From Fig. 2(a) it can be observed that the widths of both the backscattering and satellite peaks, in contrast to their positions, are sensitive to the value of the imaginary part of the dielectric function. Since the scattering geometry supports (at least) two true guided modes, the widths of these peaks are expected to grow with $\varepsilon_2(\omega)$[5]. This is much more apparent if we shift, but not scale, the tops of the enhanced backscattering peaks to the same height. We have done so by plotting $\langle \partial R/\partial\theta_s \rangle_{\rm incoh} - \langle \partial R/\partial\theta_s \rangle_{\rm incoh}\big|_{\theta_s = \theta_o}$ as a function of the scattering angle θ_s for various values of ε_2, and the results are shown in Fig. 4 for the backscattering peaks [Fig. 4(a)] and the satellite peaks [Fig. 4(b)]. Figure 4(a) clearly shows that the width of the enhanced backscattering peak increases as the imaginary part of the dielectric constant increases. Or, in other words, the enhanced backscattering peak becomes narrower and taller when the amplification of the medium is increased. This behavior is in qualitative agreement with the experimental results reported recently by Gu and Peng.[6] This finding can theoretically be understood as follows: It can be shown that the enhanced backscattering peak should have a Lorentzian form of total width[5]

$$\Delta_T(\omega) = \Delta_\epsilon(\omega) + \Delta_{\rm sc}(\omega), \tag{3.1}$$

where $\Delta_\epsilon(\omega)$ is the contribution to the width from the attenuation or amplification of the guided waves, while $\Delta_{\rm sc}(\omega)$ is the broadening due to the scattering of such waves by the surface roughness. Moreover, it can be shown that[5]

$$\Delta_\epsilon(\omega) \propto \varepsilon_2. \tag{3.2}$$

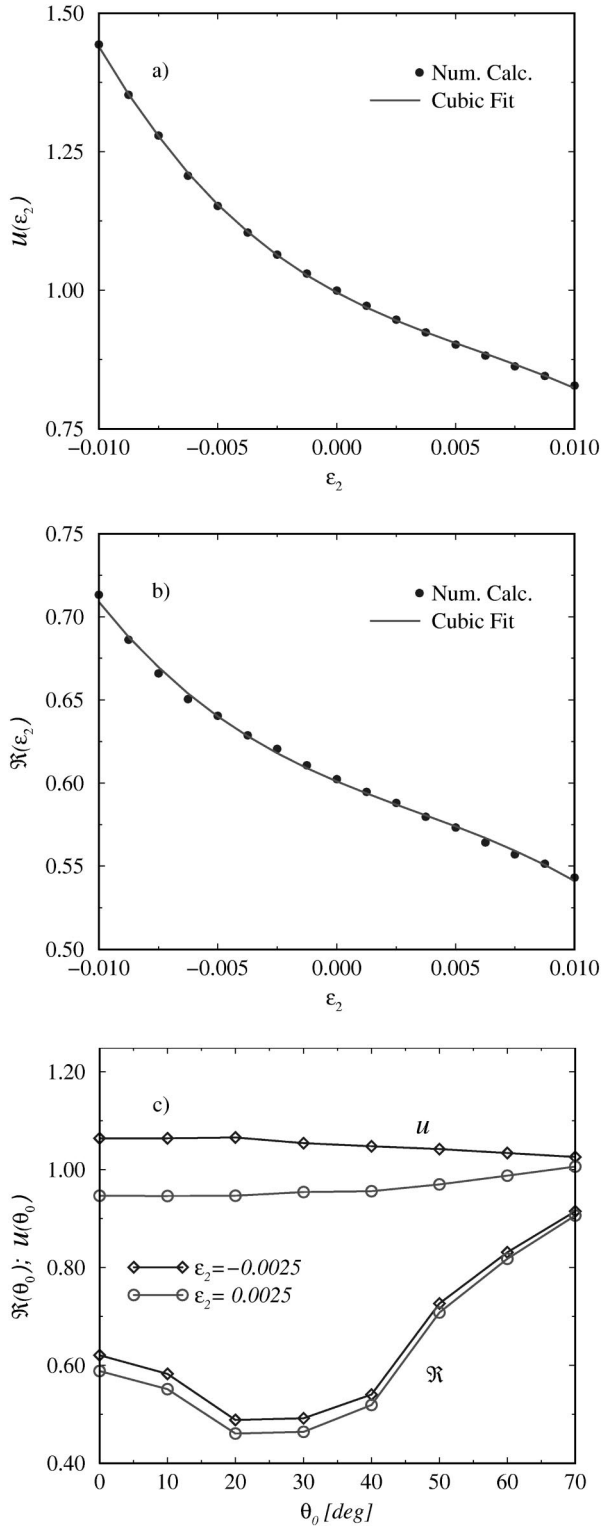

FIG. 3. The total scattered energy $\mathcal{U}$ [Eq. (2.9)] and the reflectance $\mathcal{R}$ [Eq. (2.8)] as functions of the imaginary part of the dielectric constant [(a) and (b)] and of the angle of incidence (c). In (a) and (b) the angle of incidence was $\theta_0 = 0°$, while in (c) the imaginary part of the dielectric constant was $\varepsilon_2 = \pm 0.0025$. The remaining parameters are as given in Fig. 2.

Depending on the geometrical and dielectric parameters of the film, the total width $\Delta_T(\omega)$ can be dominated by either $\Delta_\epsilon(\omega)$ or $\Delta_{sc}(\omega)$. For the parameters considered in this study, however, it is expected[5] that $\Delta_{sc}(\omega) > |\Delta_\epsilon(\omega)| > 0$. Therefore, the width should increase with increasing values of the imaginary part of the dielectric constant.

We will now examine how the full width $W(\varepsilon_2)$ of the backscattering peak depends on ε_2. In Fig. 5 we present $W(\varepsilon_2)$ vs ε_2, as obtained from the numerical simulation results shown in Fig. 2. The width of an enhanced backscatter-

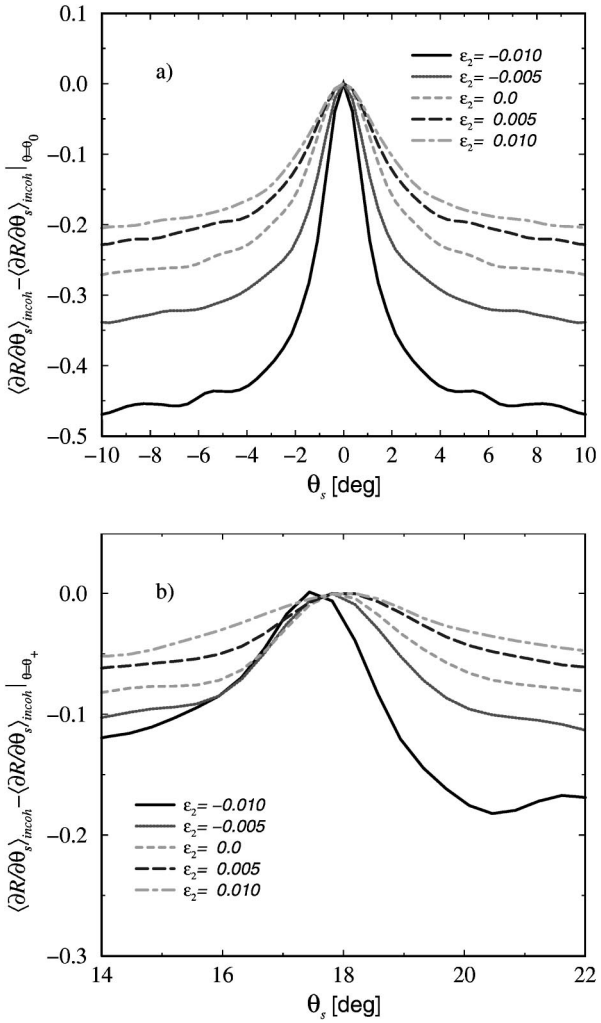

FIG. 4. Shifted plot for the mean DRC around the enhanced backscattering peak (a) and satellite peaks (b). The quantities that are plotted is $\langle \partial R/\partial\theta_s \rangle_{\text{incoh}} - \langle \partial R/\partial\theta_s \rangle_{\text{incoh}}|_{\theta_s=\theta_o}$ for the backscattering peaks and $\langle \partial R/\partial\theta_s \rangle_{\text{incoh}} - \langle \partial R/\partial\theta_s \rangle_{\text{incoh}}|_{\theta_s=\theta_+}$ for the satellite peaks, where θ_+ is the (positive) angular position of the satellite peaks.

ing peak was defined as its full width at half maximum above the background at the position of the peak. Here the background was defined to be located at the minimum value of $\langle \partial R/\partial\theta_s \rangle_{incoh}$ between the backscattering and satellite peaks. Even though the data in Fig. 5 are somewhat noisy, a linear dependence (solid curve) on ε_2, as predicted by Eq. (3.2), is easily seen.

In Fig. 4(b) we present the same kind of plot as in Fig. 4(a), but now for a satellite peak. One sees the that the width of the satellite peaks increases with increasing ε_2, the same behavior found for the enhanced backscattering peak. However, more interesting is the apparent change in the position of the satellite peaks with the value of the imaginary part of the dielectric constant. To the precision of the numerical calculations, the positions of the satellite peaks for an absorbing film ($\varepsilon_2>0$) seem to shift to larger scattering angles (in absolute value) as compared to the position of the satellite

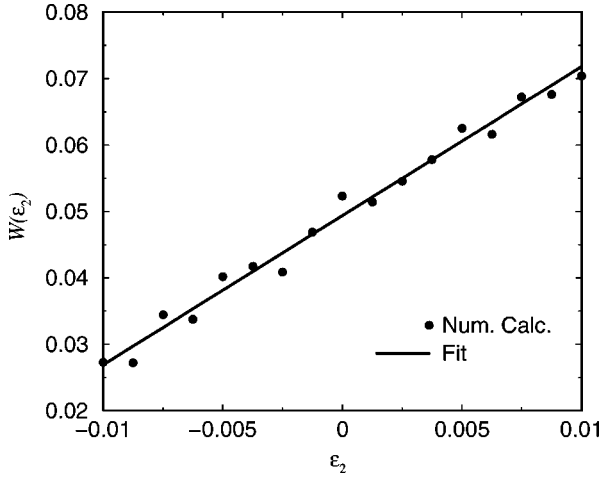

FIG. 5. The full width $W(\varepsilon_2)$ (filled dots) at half maximum above the background at its position of the backscattering peak as a function of the imaginary part ε_2 of the dielectric constant of the film as obtained from the numerical simulation results of Fig. 2. The solid line represents a linear fit in ε_2 to the numerical data.

peaks when $\varepsilon_2=0$. The opposite seems to hold true for an amplifying film ($\varepsilon_2<0$). There are two reasons for this behavior of the satellite peaks. First, the real part of the self-energy has a linear in ε_2 contribution, thus, in the presence of surface roughness the values of the wave numbers of the guided waves acquire a contribution linear in ε_2. The second reason is the strong dependence of the background intensity on the values of ε_2. The increase of the background intensity also shifts the visual positions of the satellite peaks to smaller scattering angles. For the widths of the satellite peaks, the quality of the numerical data, unfortunately, did not allow us to obtain reliable results.

IV. CONCLUSIONS

By numerical simulations we have studied light scattered from an absorbing or amplifying dielectric film deposited on the planar surface of a semi-infinite perfect conductor where the vacuum-dielectric interface is randomly rough. It has been shown that the reflectance $\mathcal{R}(\theta_0,\varepsilon_2)$, as well as the total scattered energy $\mathcal{U}(\theta_0,\varepsilon_2)$, are decreasing functions of the imaginary part of the dielectric function of the film for a fixed angle of incidence. Furthermore, it has been demonstrated that $\mathcal{U}(\theta_0,\varepsilon_2)$ is a monotonically increasing or decreasing function of the angle of incidence for fixed positive and fixed negative values of the imaginary part of the dielectric function, respectively. However, for the reflectance we find that $\mathcal{R}(\theta_0,\varepsilon_2)$ first decreases to a minimum near $\theta_0 = 25°$ and then increases. This minimum is a result of the leaky guided wave supported by the scattering structure. Moreover, for an amplifying surface both $\mathcal{R}(\theta_0,\varepsilon_2)$ and $\mathcal{U}(\theta_0,\varepsilon_2)$ are smaller then their absorbing equivalents for all angles of incidence.

The width of the enhanced backscattering peaks, as well as the satellite peaks supported by the scattering system, are

found to increase with increasing ε_2. While the location of the enhanced scattering peaks seems to be unaffected by the value of the imaginary part of the dielectric constant of the film, the corresponding positions for the satellite peaks are found to be shifted toward larger (smaller) scattering angles for positive (negative) values of the imaginary part of the dielectric function, respectively. Finally, it is found that the width of the enhanced backscattering peak is a linear function in ε_2.

ACKNOWLEDGMENTS

I. S. would like to thank the Research Council of Norway (Contract No. 32690/213) and Norsk Hydro ASA for financial support. The research of I. S., A. A. M., and T. A. L. was supported in part by Army Research Office Grant No. DAAG 55-98-C-0034. This work has also received support from the Research Council of Norway (Program for Supercomputing) through a grant of computer time.

[1] V. Freilikher, M. Pustilnik, and I. Yurkevich, Phys. Rev. B **56**, 5974 (1997).
[2] D. S. Wiersma and A. Lagendijk, Phys. World **10**, 33 (1997).
[3] D. S. Wiersma, M. P. van Albada, and A. Lagendijk, Phys. Rev. Lett. **75**, 1739 (1995).
[4] M. Kempe, G. A. Berger, and A. Z. Genack, in *Handbook of Optical Properties*, edited by R. E. Hummer and P. Wissman (CRC Press, Boca Raton, FL, 1997), Vol. II, pp. 301–330.
[5] A. V. Tutov, A. A. Maradudin, T. A. Leskova, A. P. Mayer, and J. A. Sánchez-Gil, Phys. Rev. B **60**, 12 692 (1999).
[6] Zu-Han Gu and G. D. Peng, Opt. Lett. **25**, 375 (2000).
[7] I. Simonsen and A. A. Maradudin, Opt. Commun. **162**, 99 (1999).
[8] C. S. West and K. A. O'Donnell, J. Opt. Soc. Am. A **12**, 390 (1995).
[9] A. A. Maradudin, T. Michel, A. R. McGurn, and E. R. Méndez, Ann. Phys. (N.Y.) **203**, 255 (1990).
[10] V. Freilikher, E. Kanzieper, and A. A. Maradudin, Phys. Rep. **288**, 127 (1997).
[11] F. Toigo, A. Marvin, V. Celli, and N. R. Hill, Phys. Rev. B **15**, 5618 (1977).
[12] W. H. Press, S. A. Teukolsky, W. T. Vetterling and B. P. Flannery, *Numerical Recipes*, 2nd ed. (Cambridge University Press, Cambridge, 1992).